Journal of Organometallic Chemistry, 478 (1994) 57–65

A density functional study on σ-bond metathesis reactions of possible importance in dehydrogenative silane polymerization

Tom Ziegler and Elzbieta Folga

Department of Chemistry, University of Calgary, Calgary, Alta. T2N 1N4 (Canada)

(Received August 17, 1993; in revised form October 7, 1993)

Abstract

Possible elementary reaction steps in dehydrogenative polymerization of silanes have been studied by nonlocal density functional calculations. The reaction steps involve silylation $L_nM\text{-}H + SiH_4 \rightarrow L_nM\text{-}SiH_3 + H_2$ (1), and the silicon–silicon bond forming step, $L_nM\text{-}SiH_3 + SiH_4 \rightarrow L_nM\text{-}H + Si_2H_6$ (2). For the model system $L_nM = Cl_2Sc$, step (1) has a calculated enthalpy of 3 kJ/mol and a calculated activation energy of 7 kJ/mol whereas step (2) has an enthalpy of 10 kJ/mol and a negative activation energy of −11 kJ/mol. It is concluded that the mechanism proposed in the literature for dehydrogenative polymerization of silanes in terms of the steps (1) and (2) is feasible for $L_nM = Cp_2M$ with M = Sc, Y, La, Lu and Sm. Studies were also carried out on the corresponding steps involving carbon rather than silicon. It was found that the carbon–carbon bond forming process analogous to (2) has an activation energy of 132 kJ/mol and it is suggested that the reaction between $L_nM\text{-}CH_3$ and CH_4 instead leads to the methyl exchange process $L_nM\text{-}CH_3 + CH_4 \rightarrow L_nM\text{-}CH_3 + CH_4$ with an activation energy of 33 kJ/mol for $L_nM = Cl_2Sc$.

Key words: Scandium; Silane; Polymerization; Metathesis reaction; Density functional theory

1. Introduction

The dehydrogenative polymerisation of silanes

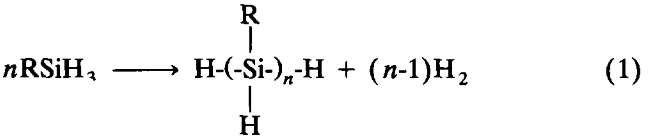

$$n\mathrm{RSiH_3} \longrightarrow \mathrm{H(\text{-}\overset{\displaystyle R}{\underset{\displaystyle H}{Si}}\text{-})_{\mathit{n}}\text{-}H} + (n-1)\mathrm{H_2} \qquad (1)$$

is a mildly endothermic process ($\Delta H \sim 15$ kJ/mol) that can be driven by the removal of H_2 and catalysed by electron poor metal centers as first demonstrated by Harrod [1]. A number of mechanisms have been suggested for catalytic polymerization of silanes [2]. Marks [3] and Tilley [4] recently proposed a mechanism (Scheme 1) based on σ-bond metathesis involving four-center bond transpositions, **1a** and **1b** in Scheme 1.

The transition state **1a** in Scheme 1 has a hydrogen in the position diagonal to the metal center. Such a transition state is implicated in many analogous reactions involving carbon, notably the well studied hydrogenation reaction 5 of eqn. (2) where M = Sc, Y, and Lu.

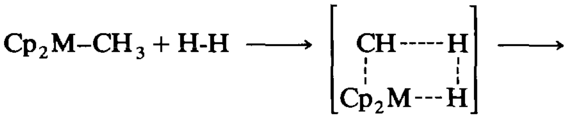

(2a)

$$Cp_2M\text{-}CH_3 + H\text{-}H \longrightarrow \left[\begin{matrix} CH\text{-----}H \\ \vdots \qquad \vdots \\ Cp_2M\text{---}H \end{matrix}\right] \longrightarrow Cp_2M\text{-}H + H\text{-}CH_3 \qquad (2)$$

It is in general assumed [5a] that the barrier in eqn. (2) is low since the spherical 1s orbital on the hydrogen diagonal to M in the transition state **2a** can interact well with orbitals on the adjacent (H and CH_3) groups, and similar considerations apply to **1a**.

The transition state **2b** with a Group 14 element in the diagonal position has not been invoked in analogous carbon chemistry since the σ-orbital on the CH_3 fragment is considered to be too directional to interact effectively with both adjacent groups, as opposed to the spherical 1s hydrogen orbital in **1a**. In support of this view [5a], the reaction between $Cp_2M\text{-}CH_3$ and $H\text{-}C'H_3$ does not produce any ethane according to

---

Correspondence to: Professor T. Ziegler.

0022-328X/94/\$7.00
SSDI 0022-328X(93)24245-Z

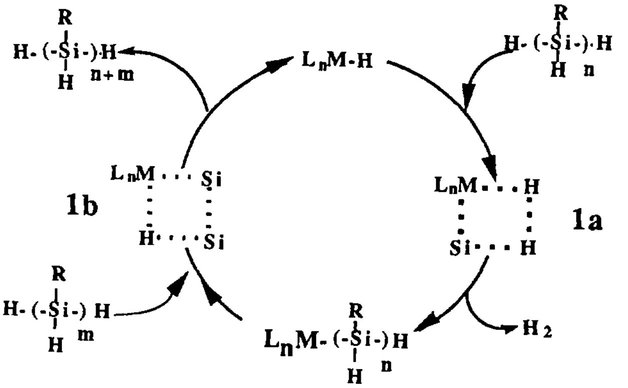

Scheme 1.

eqn. (3) with the supposedly unfavourable transition state **2b**.

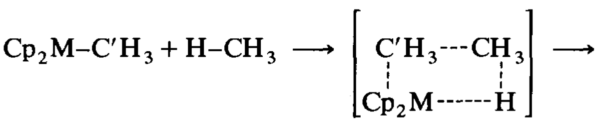

$$Cp_2M{-}C'H_3 + H{-}CH_3 \longrightarrow \left[\begin{array}{c} C'H_3{-}{-}{-}CH_3 \\ \vdots \qquad \vdots \\ Cp_2M{-}{-}{-}{-}{-}{-}H \end{array}\right] \longrightarrow$$

(2b)

$$Cp_2M{-}H + C'H_3{-}CH_3 \quad (3)$$

Instead, $Cp_2M{-}C_3$ and $H{-}C'H_3$ react according to eqn. (4) in the methyl exchange reaction first discovered by Watson [5b] for M = Lu. This process has the supposedly more favorable transition state **2c** with H in the diagonal position.

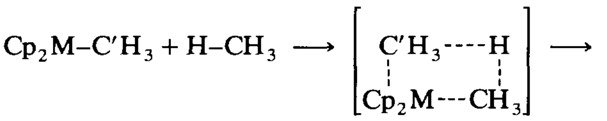

$$Cp_2M{-}C'H_3 + H{-}CH_3 \longrightarrow \left[\begin{array}{c} C'H_3{-}{-}{-}{-}H \\ \vdots \qquad \vdots \\ Cp_2M{-}{-}{-}CH_3 \end{array}\right] \longrightarrow$$

(2c)

$$Cp_2M{-}CH_3 + H{-}CH_3 \quad (4)$$

The question we would like to answer is whether **2b** is in fact of much higher energy than **2c**? If so, does the replacement of a carbon atom with silicon help to make the two transition states analogous to **2c** and **2b** more similar in energy? We shall further study the transition states **1a** and **2a** in order to assess how the replacement of carbon by silicon influences the energy barrier for the associated hydrogenolysis processes.

It is the objective of the present study to assess whether the two σ-bond metathesis steps proposed for the dehydrogenative polymerization of silanes [2,3] in Scheme 1 are feasible. We shall, in particular, evaluate the barriers associated with the two transition states **1a** and **1b**. The Cp_2M fragment will be modelled by $ScCl_2$. We have previously carried out studies on σ-bond metathesis steps involving carbon as well as the Cl_2Lu [6] and Cp_2Sc [7] metal fragments. The processes in eqns. (2) and (4) have been studied previously as discussed in [7]. Calculations on the process in eqn. (3) as well as the silicon analogues to the reactions in eqs. (2)–(4) have not been presented previously.

Our calculations are based on approximate density functional theory (DFT) [8] which over the past decade has emerged as a tangible and versatile computational method. The recently acquired popularity of approximate DFT stems in large measure from its computational expedience which makes it amenable even to large size molecules in a fraction of the time required for HF or post-HF calculations. More importantly, perhaps, is the fact that expectation values derived from approximate DFT in most cases are better in line with experiment than results obtained from HF calculations. This is in particular the case for systems involving transition metals. An analysis of why approximate DFT affords more reliable results than HF has recently been published by Cook and Karplus [9] as well as Tschinke and Ziegler [10].

2. Computational details

The reported calculations were all carried out by utilizing the ADF program system developed by Baerends *et al.* [11] and vectorized by Ravenek [11c]. The numerical integration procedure applied is due to Becke [12]. The geometry optimization procedure was based on the method proposed by Versluis and Ziegler [13]. The electronic configurations of the molecular systems were described by an uncontracted triple-ζ STO basis set [14] on scandium for the 3s, 3p, 3d, 4s and 4p sub-shells, as well as a double-ζ STO basis set [14] on chlorine (3s, 3p), silicon (3s, 3p), carbon (2s, 2p) and hydrogen (1s). The basis set was augmented with a single 3d orbital for carbon, chlorine and silicon as well as a 2p function for hydrogen. The $1s^22s^22p^6$ configuration on Sc, the $1s^2$ configuration on carbon and the $1s^22s^22p^6$ configuration on Cl and Si were assigned to the core and treated by the frozen-core approximation [11]. A set of auxiliary [15] s, p, d, f and g STO functions, centered on the different nuclei, was used in order to fit the molecular density and present the Coulomb and exchange potentials accurately in each SCF cycle.

Energy differences were calculated by augmenting the local density approximation (LDA) energy expression by Vosko *et al.* [16a] with Becke's [16b] exchange corrections and Perdew's [16c] nonlocal correlation correction. Calculations on metal carbonyls [17], binuclear metal complexes [18], alkyl and hydride complexes [18c,19] as well as complexes containing M–L bonds for a number of different ligands [20] have shown that the approximate DF method employed here afford metal–ligand and metal–metal bond energies of nearly chemical accuracy (± 5 kcal mol^{-1}). More than 100 molecular structures optimized by approximate density functional theory have been compared with experiment [8c,13,18c,21]. The method has also been applied to elementary reaction steps in organic [22] and organometallic [23] chemistry. The agreement between experiment and theory is in most cases excellent. The application of approximate density functional theory to organometallic chemistry has been reviewed recently [24]. It is not possible with the available computational resources to calculate frequencies for all the optimized structures presented in this study since force constant calculations at the moment are carried out by numerical differentiation of the analytical gradients. This will change when analytical second derivatives become available.

3. Results and discussions

In the following, we discuss the energy profiles for the hydrogenolysis reaction of eqn. (2) involving both silicon, **1a**, and carbon, **2a**, as well as the X–X bond forming process of eqn. (3) with X = Si, **1b**, and X = C, **2b**. Profiles are also be presented for the exchange process of eqn. (4). All the profiles are based on the calculated bond energies presented in Table 1. It is clear from this table that the X–X and X–H bond energies with X = C and Si are within 20 kJ/mol of experiment [25]. Experimental data are not available for the Sc–H and Sc–XH_3 bond energies. However, we expect the relative Sc–H and Sc–XH_3 bond energies, which are of importance for the profiles, to be accurate to within 20 kJ/mol. The Sc–H and Sc–XH_3 bond energies calculated with Cp_2Sc as a fragment instead of Cl_2Sc were found [7] in a previous study to be ~ 40 kJ/mol higher in energies. However, the relative energies are quite similar.

TABLE 1. Calculated and experimental bond energies [a]

Compound	Bond	Bond energies			
		Calculated		Experiment	
		D_e	D_0	D_e	D_0
H_2	H-H	465	444	463 [b]	432 [b]
CH_4	C-H	449	415	468 [c]	431 [d]
C_2H_6	C-C	400	363		367 [e]
SiH_4	Si-H	396	381		384 [f]
Si_2H_6	Si-Si	314	299		308 [g]
Cl_2ScH	Sc-H	291			
Cl_2ScCH_3	Sc-CH_3	267			
Cl_2ScSiH_3	Sc-SiH_3	219			

[a] Energies in kJ/mol. D_e is the electronic bond dissociation energy. D_0 includes zero point vibrational energy corrections. [b] Ref. 25a. [c] Ref. 25b. [d] Ref. 25c. [e] Ref. 25d. [f] Ref. 25e. [g] Ref. 25f.

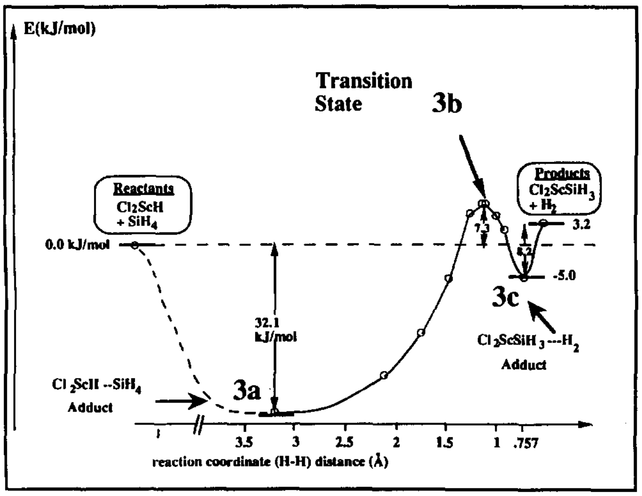

Fig. 1. Reaction profile for the silylation process, $Cl_2Sc{-}H + SiH_4 \rightarrow Cl_2Sc{-}SiH_3 + H_2$.

3.1. *The methylation and silylation reactions*

The profile for the silylation reaction

$$Cl_2Sc{-}H + SiH_4 \longrightarrow H_2 + Cl_2Sc{-}SiH_3 \qquad (5)$$

is displayed in Fig. 1. The profile was obtained by changing the distance between the hydrogens of the Sc–H and Si–H bonds involved in the metathesis reaction, while optimizing all other degrees of freedom.

An adduct, **3a**, between Cl_2ScH and SiH_4 is formed early on in the reaction with a complexation energy of 32 kJ/mol. The process proceeds to the transition state, **3b**, with a total barrier of 39 kJ/mol from **3a** or 7 kJ/mol from the reactants, $Cl_2ScH + SiH_4$. The four center transition state, **3b**, exhibits a Si–H bond stretched by 0.16 Å compared to the equilibrium Si–H distance in **3a**. The weakened Si–H interaction is offset by the formation of a Sc–Si bond as well as a H–H interaction.

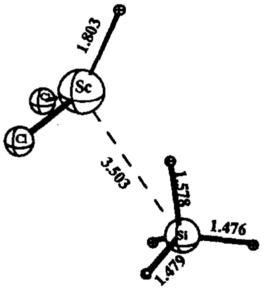

3a

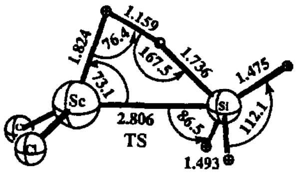

3b

On the product side, a weak adduct, **3c**, is formed between H_2 and Cl_2ScSiH_3. Only 5 kJ/mol is required to dissociate **3c** into H_2 and Cl_2ScSiH_3. The process of

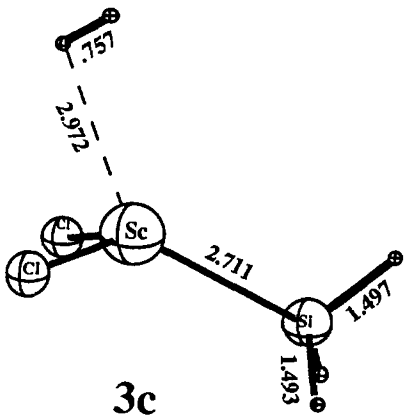

3c

eqn. (5) has an endothermicity of 3 kJ/mol (Fig. 1). It follows from Table 1 that the loss of a Sc–H bond in place of the weaker Sc–SiH_3 link is balanced by the formation of a strong H–H link at the expense of the weaker Si–H bond.

A schematic representation of the profile for the corresponding methylation process is given in Fig. 2. Again a strong adduct, **4a**, is formed in the initial stages of the reaction, now between Cl_2ScH and CH_4. The complexation energy is 42 kJ/mol. The reaction goes over a barrier of 54 kJ/mol from **4a** or 12 kJ/mol from the reactants (Fig. 2). The C–H bond involved in the σ-metathesis is completely broken at the transition state **4b**, and replaced by a nearly full Sc–C bond as well as a H–H bond stretch to 0.90 Å

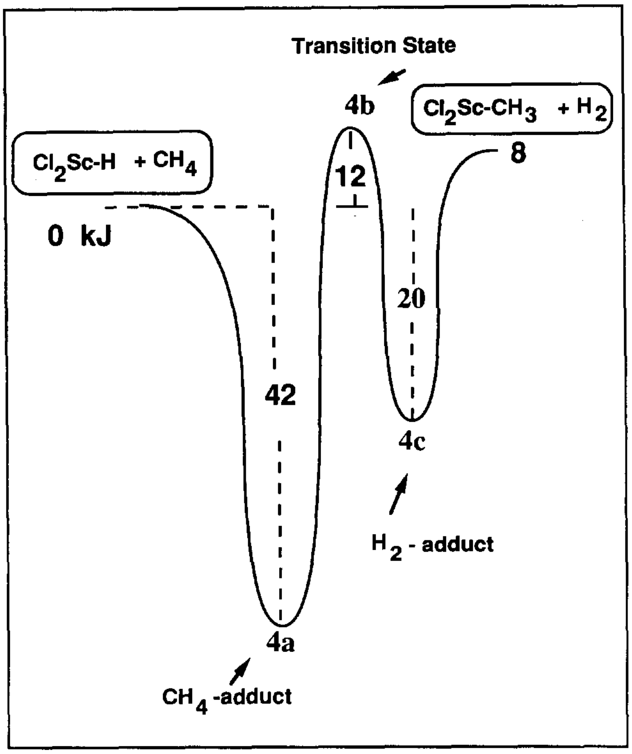

Fig. 2. Reaction profile for the methylation process, $Cl_2Sc\text{–}H + CH_4 \rightarrow Cl_2Sc\text{–}CH_3 + H_2$.

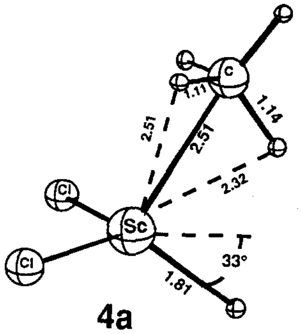

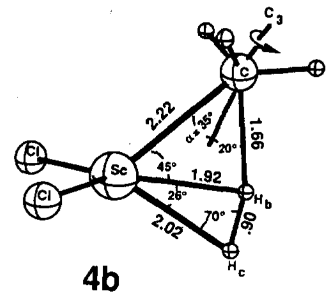

The final step of the reaction produces a weak adduct between H_2 and Cl_2ScCH_3 (**4c**) before dissociation of H_2. The process is modestly endothermic by 8 kJ/mol (Fig. 2). It follows from Table 1 that energy required to replace a Sc–H bond by the weaker Sc–CH_3 link is counterbalanced by the gain of a H–H bond in place of the weaker C–H link.

The modest activation barrier of 7 kJ/mol as well as the negligible endothermicity of 3 kJ/mol for the model reaction of eqn. (5) clearly indicate that the silylation process of Scheme 1 is a viable reaction step. We find further, in agreement with experiment [5] and previous calculations [6a,7], that the corresponding methylation process is quite facile.

3.2. The carbon–carbon and silicon–silicon bond forming metathesis processes

We have also modelled the Si–Si bond forming step, **1b**, in Scheme 1 by considering the metathesis reaction

$$Cl_2Sc\text{–}SiH_3 + SiH_4 \longrightarrow Cl_2Sc\text{–}H + Si_2H_6 \qquad (6)$$

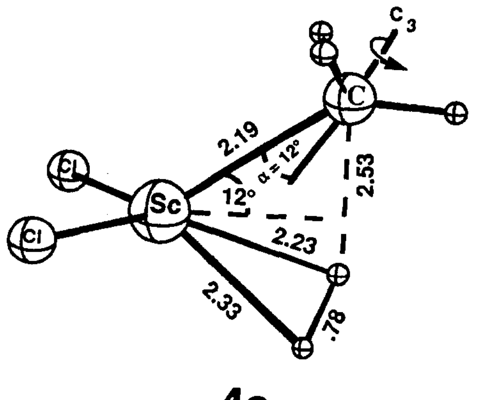

4c

The energy profile for the process in eqn. (6) is shown in Fig. 3. The profile in Fig. 3 was constructed by changing the Si–Si distance in steps while optimizing all other degrees of freedom.

The two reactants $Cl_2Sc{-}SiH_3$ and SiH_4 are seen to form a weak adduct **5a** at the start of the process in eqn. (6) with a complexation energy of 20 kJ/mol. The stability of **5a** is primarily due to an agostic interaction between the metal center and one of the Si–H bonds on the approaching SiH_4. The process proceeds towards the transition state **5b** with a modest barrier of 9 kJ/mol relative to the adduct **5a**.

At the transition state, the silyl group has rotated its C_3 axis by an angle α, **5b**. The rotation takes place from a direction pointing towards the metal center at $\alpha = 0°$ to an orientation at $\alpha = 49°$ where the C_3 axis and the SiH_3 σ-orbital directed along this axis are pointing towards the silicon center of the incoming SiH_4 molecule in anticipation of a Si–Si bond formation. At the transition state, the Si–Si distance of $R(Si{-}Si) = 3.15$ Å is still much longer than the Si–Si distance in Si_2H_6 of $R(Si{-}Si) = 2.28$ Å. The rotation of the C_3 axis by $\alpha = 49°$ will weaken the $Sc{-}SiH_3$ interaction and thus give rise to an energy barrier. However, the loss in $Sc{-}SiH_3$ interaction at **5b** is compensated for by the formation of an agostic interaction between scandium and one of the silyl hydrogens, H_b, with a $R(Sc{-}H_b)$ interaction distance of 2.02 Å, which is only 0.2 Å longer than a regular Sc–H bond, **5a**. At the incoming SiH_4 one of the hydrogens, H_a, forms a strong agostic interaction with scandium resulting in a $Sc{-}H_a$ distance of $R(Sc{-}H_a) = 1.94$ Å, which is only 0.12 Å longer than a full Sc–H bond. At the same time, the $Si{-}H_a$ distance has increased from 1.48 Å in free SiH_4 to 1.54 Å in **5b**. The agostic interaction between scandium and H_a is also instrumental in keeping the activation barrier low (Fig. 3).

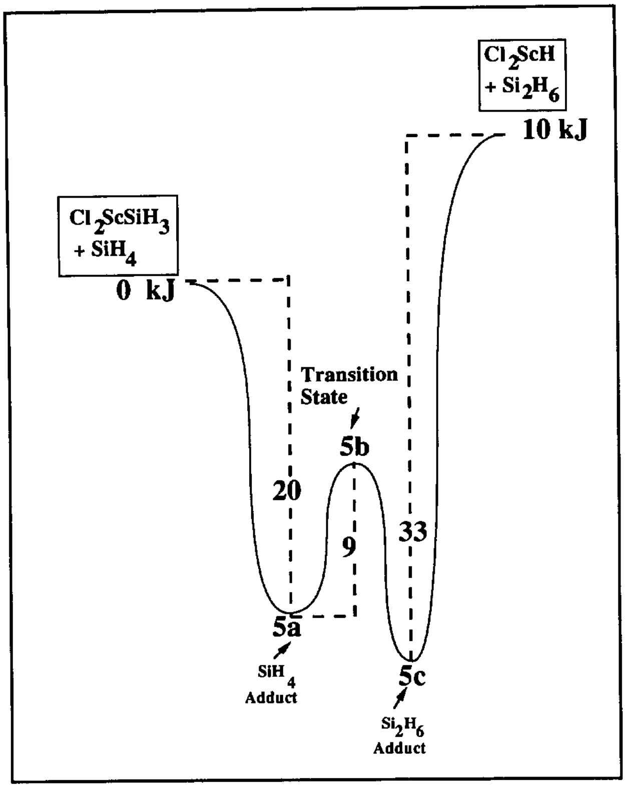

Fig. 3. Reaction profile for the silicon–silicon bond forming process, $Cl_2Sc{-}SiH_3 + SiH_4 \rightarrow Cl_2Sc{-}H + Si_2H_6$.

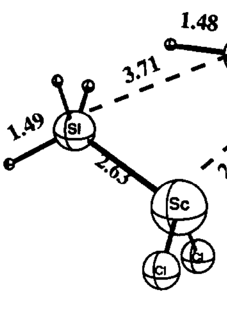

5a

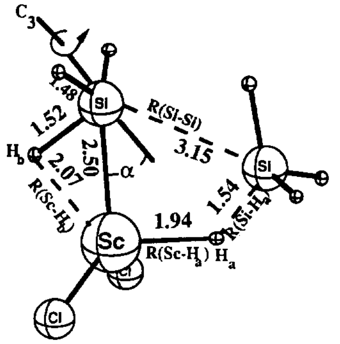

5b

The reaction proceeds smoothly from **5b** to the $Cl_2ScH + Si_2H_6$ addut **5c** by a shortening of $R(Si{-}Si)$ accompanied by a further increase of α to 66° and a gradual rupture of the $Si{-}H_a$ bond while the $Sc{-}H_a$ interaction is strengthed. The agostic $Sc{-}H_b$ interaction is maintained throughout the **5b** to **5c** transit, and largely responsible for the stability of **5c** compared to the $Cl_2ScH + Si_2H_6$ products. The transition state **5b** as well as the two intermediates **5a** and **5c** are all of lower energy than the reactants $Cl_2Sc{-}CH_3 + SiH_4$. Thus, the process in eqn. (6) has formally a negative activation energy.

The process in eqn. (6) is nearly thermoneutral with an endothermicity of 10 kJ/mol. It is clear from Table 1 that the formation of a weak Si–Si bond at the expense of a stronger Si–H link is offset by the formation of the strong Sc–H bond in place of the weaker Sc–Si link. Thus, the Si–Si bond forming step is quite feasible from a thermodynamic point of view. We have further seen from Fig. 3 that the process is kinetically viable.

We have modelled the corresponding carbon–carbon bond forming step by the analogous process

$$Cl_2Sc{-}CH_3 + CH_4 \longrightarrow Cl_2Sc{-}H + C_2H_6 \qquad (7)$$

for which we present the reaction profile in Fig. 4.

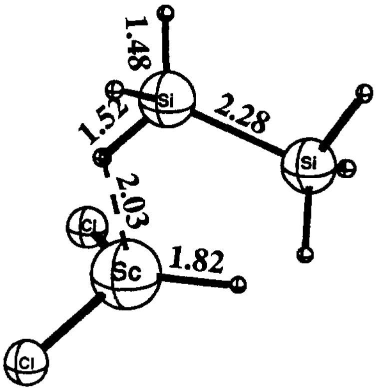

5c

The carbon–carbon bond forming process has a substantial activation barrier of 132 kJ/mol. The transition state structure **6b** exhibits many features that are similar to the corresponding transition state for the analogous silicon–silicon bond forming process of eqn. (6), **5b**. Thus, the C_3 axis on the methyl group is rotated by 30° in order to direct the σ-orbital towards the carbon center of the incoming CH_4 molecule. The rotation will cause a reduction in the methyl–scandium interaction. This destabilization is to some degree countered by an agostic interaction between H_2 and scandium resulting in a stretch of the C–H_2 distance to 1.21 Å. The incomming CH_4 molecule is interacting with scandium through one of the hydrogens, H_1. The Sc–H_a distance is already quite short with R(Sc–H_a) = 1.94 Å. The Sc–H_1 interaction will eventually evolve into a full Sc–H bond. The carbon–carbon distance is still large with R(C–C) = 2.15 Å.

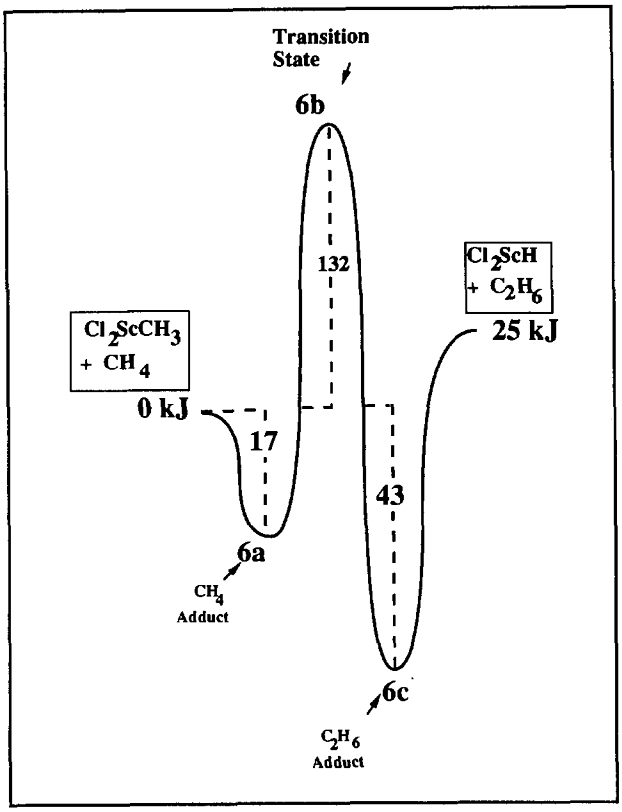

Fig. 4. Reaction profile for the carbon–carbon bond forming process, $Cl_2Sc\text{–}CH_3 + CH_4 \rightarrow Cl_2Sc\text{–}H + C_2H_6$.

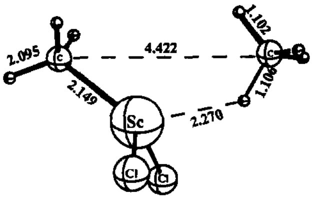

6a

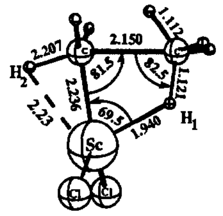

6b

The major difference between **6b** and **5b** is in the steric interactions between the hydrogens on one XH_3 group and X on the other XH_3 group. These interactions are negligible in **5b** with X = Si but quite substantial in **6b** with X = C. The destabilizing steric interaction between carbon and hydrogen atoms on adjacent methyl groups is responsible for the high barrier associated with the carbon–carbon forming process in eqn. (7). The steric interactions could be reduced by directing the C_3 axis of the two CH_3 groups towards each other. However, this would result in a reduction of the Sc–C and H–C bond strengths while producing only a weak carbon–carbon bond at R(C–C) = 2.15 Å. At the last stages of the reaction in eqn. (7), a weak adduct **6c**

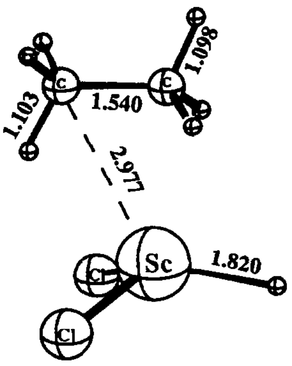

6c

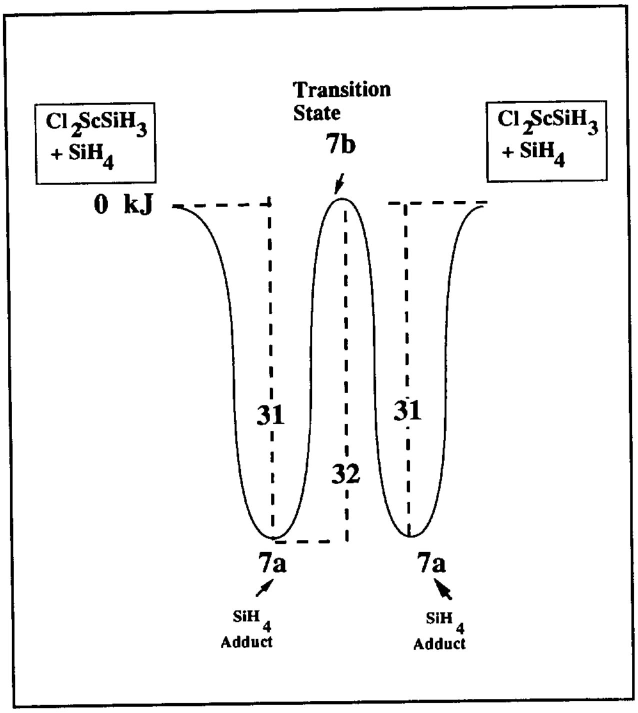

Fig. 5. Reaction profile for the silyl exchange process, $Cl_2Sc\text{-}SiH_3 + SiH_4 \rightarrow Cl_2Sc\text{-}SiH_3 + SiH_4$.

is formed. It is calculated to be 28 kJ/mol more stable than the products, Cl_2ScH and C_2H_6.

The carbon–carbon forming reaction of eqn. (7) is feasible from a thermochemical point of view with a reaction enthalpy of 25 kJ/mol (Fig. 4). However, we must conclude that it is kinetically unfavorable due to the high energy of transition state **6b**.

3.3. The methyl and silyl exchange reactions

We have included studies on the silyl exchange reaction

$$Cl_2Sc\text{-}SiH_3 + SiH_4 \longrightarrow Cl_2Sc\text{-}SiH_3 + SiH_4 \qquad (8)$$

as well as the corresponding methyl exchange process

$$Cl_2Sc\text{-}CH_3 + CH_4 \longrightarrow Cl_2ScCH_3 + CH_4 \qquad (9)$$

in order to assess how they compare to the corresponding silicon–silicon, eqn. (6), and carbon–carbon, eqn. (7), bond forming steps in terms of activation energy.

The profile for the silyl exchange reaction of eqn. (8) is displayed in Fig. 5. The initially formed adduct **7a** between $Cl_2Sc\text{-}SiH_3$ and SiH_4 has a stability of 31 kJ/mol. The adduct **7a** has two hydrogens on SiH_4 directed towards scandium as opposed to one for the similar adduct **5a** between $Cl_2Sc\text{-}SiH_3$ and SiH_4 in the silicon–silicon bond forming process of eqn. (6).

The transition state **7b** has a kite-shape involving the four centers Sc, Si_a, Si_b and H_a. One Si–H distance, $Si_a\text{-}H_a$, has been stretched from $R(\text{Si-H}) = 1.48$ Å in free SiH_4 to $R(\text{Si-H}) = 1.96$ Å in **7b**. Also the C_3-axis of the silyl group has been rotated towards the H_a atom on SiH_4 in anticipation of the $Si_b\text{-}H_a$ bond formation. The rotation has reduced the $Sc\text{-}Si_b$ bonding interaction. The transition state **7b** is stabilized by the formation of a nearly full $Sc\text{-}H_a$ bond with $R(\text{Sc-H}) = 1.96$ Å. There is in addition a partial formation of the $Sc\text{-}Si_b$ and $Si_b\text{-}H$ bonds.

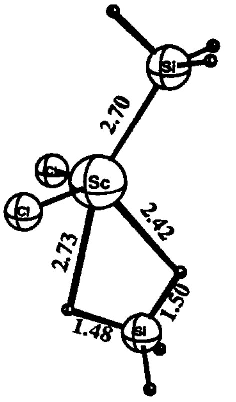

7a

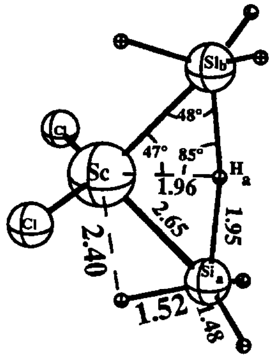

7b

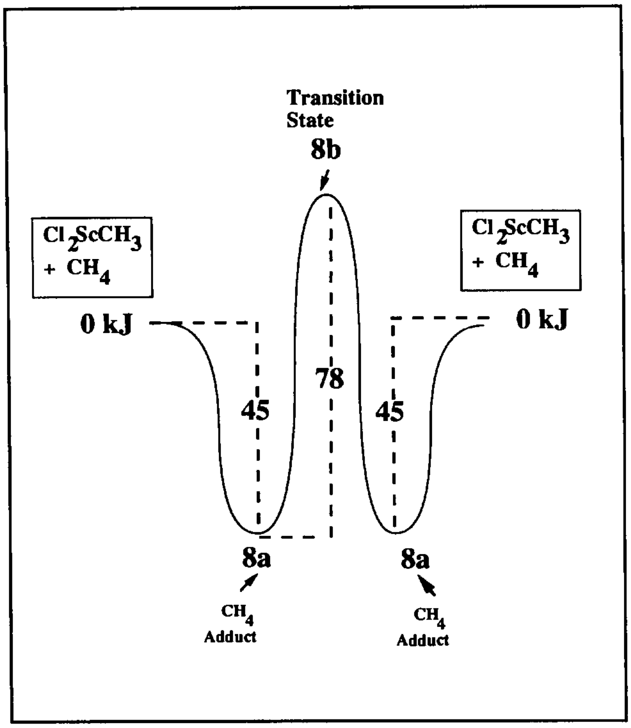

Fig. 6. Reaction profile for the methyl exchange process, $Cl_2Sc\text{-}CH_3 + CH_4 \rightarrow Cl_2Sc\text{-}CH_3 + CH_4$.

It follows from Fig. 5 that the reaction of eqn. (8) has a modest activation energy of 32 kJ/mol from **7a** or 1 kJ/mol from the reactants $Cl_2Sc-SiH_3$ and SiH_4. Thus the silyl exchange reaction is kinetically viable. However, the transition state **7b** for the silyl exchange reaction is seen to be 12 kJ/mol higher in energy than **5b** corresponding to the transition state for the silicon–silicon bond forming process of eqn. (6).

We present finally in Fig. 6 the profile for the methyl exchange process of eqn. (9). The transition state **8b** has the same kite-shape as **7b**. The C_a-H_c and C_b-H_c bonds are stretched to $R(C-H) = 1.4$ Å, and the C_3-axis of the methyl groups are directed towards the central H_c atom, thus reducing the Sc–C interactions. The transition state **8b** is stabilized by the formation of a $Sc-H_c$ bond as well as the pronounced $Sc-H_a$ and $Sc-H_b$ agostic interactions. The agostic interactions are accompained by a stretch of the $C-H_a$ and $C-H_b$ bonds to 1.21 Å.

The activation energy for the methyl exchange process is 78 kJ/mol from the intermediate **8a** and 33 kJ/mol from the reactants $Cl_2Sc-CH_3 + CH_4$ (Fig. 6). It is clear from our investigation that the reaction between Cl_2Sc-CH_3 and CH_4 will result in methyl exchange according to eqn. (9) with the transition state **8b** rather than carbon–carbon bond formation according to eqn. (7) with the transition state **6b** which is 99 kJ/mol above **8b** in energy.

4. Concluding remarks

We have investigated a proposed mechanism [3,4] for dehydrogenative polymerization of silanes based on two four-center bond transpositions, **1a** and **1b** of Scheme 1. The first transposition was modelled by the silylation reaction of eqn. (5). It was found that the silylation process is quite feasible with an activation energy of 7 kJ/mol and a reaction enthalpy of only 3 kJ/mol. The second transposition was modelled by the silicon–silicon bond forming step of eqn. (8). The process in eqn. (8) has a reaction enthalpy of 10 kJ/mol and proceeds from the adduct **5a** between $Cl_2Sc-SIH_3$ and SiH_4 with an activation energy of 9 kJ/mol.

We have used Cl_2ScH as a catalyst for the dehydrogenative polymerization of silanes through the sequence of two four-center bond transpositions represented by the σ-metathesis reactions of eqns. (5) and (8). Our catalyst has served as a model for d^0 hydrides of the type Cp_2MH where M = Sc, Y, Lu and Sm. We conclude that hydrides of the type Cp_2MH could act as catalysts for dehydrogenative polymerization of silanes according to Scheme 1 as suggested by Marks [3] and Tilley [4]. Harrod [1] and Tilley [4] have pointed to $Cp_2M(Cl)H$ with M = Ti, Zr and Hf as an other efficient series of catalysts for dehydrogenative polymerization of silanes. For $Cp_2M(Cl)H$, the sequence of bond transpositions given in Scheme 1 might be sterically more demanding, in particular for M = Ti. We are in the process of investigating dehydrogenative polymerization of silanes by $Cp_2M(Cl)H$.

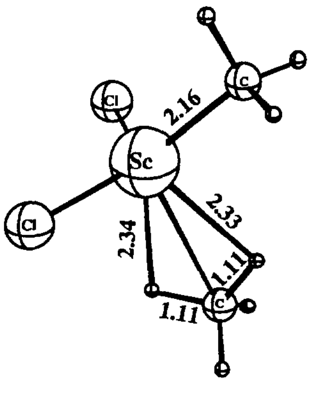

8a

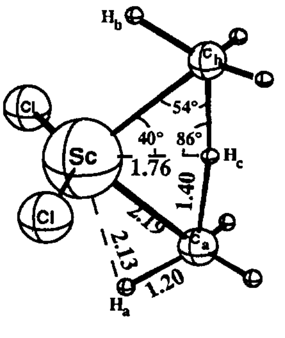

8b

Acknowledgement

This investigation was supported by the Natural Sciences and Engineering Research Council of Canada (NSERC). We gratefully acknowledge the Donors of the Petroleum Research Fund, administered by the American Chemical Society (ACS-PRF No. 27023-AC3).

References

1 J.F. Harrod and S.S. Yun, *Organometallics, 6* (1987) 1381.
2 J.F. Harrod, T. Ziegler and V. Tschinke, *Organometallics, 9* (1990) 897.
3 M.A. Giardello, W.A. King, S.P. Noland, M. Porchia, C. Sishta and T. Marks, *NATO ASI, C367* (1992) 35.
4 T.D. Tilley, *Acc. Chem. Res., 26* (1993) 22.
5 (a) M.E. Thompson, S.M. Buxter, A.R. Bukks, B.J. Burger, M.C. Nolan, B.D. Santarsiero, W.P. Schaefer and J.E. Bercaw, *J. Am. Chem. Soc., 109* (1987) 203; (b) P.L. Watson and G.W. Parshall, *Acc. Chem. Res., 18* (1985) 51.
6 (a) E. Folga and T. Ziegler, *Can. J. Chem., 70* (1992) 333; (b) E. Folga, T. Ziegler and L. Fan, *New J. Chem.*, 15 (1991) 741.
7 T. Ziegler, E. Folga and A. Berces, *J. Am. Chem. Soc., 115* (1993) 636.
8 (a) R.G. Parr and W. Yang, *Density-Functional Theory of Atoms and Molecules*, Oxford University Press, New York, 1989; (b) E.S. Kryachko and E.V. Ludena, *Density Functional Theory of Many Electron Systems*, Kluwer, Dordrecht, 1991; (c) T. Ziegler, *Chem. Rev., 91* (1991) 651; (d) A.D. Becke, *Int. J. Quantum Chem., S23* (1989) 599.
9 M. Cook and M. Karplus, *J. Phys. Chem., 91* (1987) 31.
10 V. Tschinke and T. Ziegler, *J. Chem. Phys., 93* (1990) 8051.

11 (a) E.J. Baerends, D.E. Ellis and P. Ros, *Chem. Phys.*, *2* (1973) 41; (b) E.J. Baerends, Ph.D. Thesis, Vrije Universiteit, Amsterdam, 1975; (c) W. Ravenek, in J.J.J. te Riele, Th.J. Dekker and H.A. van de Vorst (eds.), Algorithms and Applications on Vector and Parallel Computers, Elsevier, Amsterdam, 1987.

12 A.D. Becke, *J. Chem. Phys.*, *88* (1988) 2547.

13 L. Versluis and T. Ziegler, *J. Chem. Phys.*, *88* (1988) 322.

14 (a) G.J. Snijders, E.J. Baerends and P. Vernooijs, *Atomic Nucl. Data Tables*, *26* (1982) 483; (b) P. Vernooijs, G.J. Snijders and E.J. Baerends, Slater type basis functions for the whole periodic system, Internal report, Free University of Amsterdam, The Netherlands, 1981.

15 J. Krijn and E.J. Baerends, Fit functions in the HFS-method, Internal report, Free University, Amsterdam, The Netherlands, 1984 (in Dutch).

16 (a) S.H. Vosko, L. Wilk and M. Nusair, *Can. J. Phys.*, *58* (1990) 1200; (b) A.D. Becke, *Phys. Rev. A*, *38* (1988) 2398; (c) J.P. Perdew, *Phys. Rev. B*, *33* (1986) 8822; *34* (1986) 7406.

17 T. Ziegler, V. Tschinke and C. Ursenbach, *J. Am. Chem. Soc.*, *109* (1987) 4825.

18 (a) T. Ziegler, V. Tschinke and A. Becke, *Polyhedron*, *6* (1987) 685; (b) H. Jacobsen, H.B. Kraatz, T. Ziegler and P.M. Boorman, *J. Am. Chem. Soc.*, *114* (1992) 7851; (c) E. Folga and T. Ziegler, *J. Am. Chem. Soc.*, *115* (1993) 5169.

19 (a) T. Ziegler, V. Tschinke and A. Becke, *J. Am. Chem. Soc.*, *109* (1987) 1351; (b) T. Ziegler, W. Cheng, E.J. Baerends and W. Ravenek, *Inorg. Chem.*, *27* (1988) 3458; (c) T. Ziegler, V. Tschinke, E.J. Baerends, J.G. Snijdes and W. Ravenek, *J. Phys. Chem.*, *93* (1989) 3050.

20 (a) H.B. Kraatz, H. Jacobsen, T. Ziegler and P.M. Boorman, *Organometallics*, *12* (1993) 76; (b) T. Ziegler, V. Tschinke, L. Versluis and E.J. Baerends, *Polyhedron*, *7* (1988) 1625.

21 L. Fan and T. Ziegler, *J. Chem. Phys.*, *95* (1991) 7401.

22 (a) L. Fan and T. Ziegler, *J. Am. Chem. Soc.*, *114* (1992) 10890; (b) L. Deng and T. Ziegler, *J. Chem. Phys.*, *99* (1993) 3823; (c) L. Fan and T. Ziegler, *J. Chem. Phys.*, *92* (1990) 897.

23 (a) L. Versluis and T. Ziegler, *Organometallics*, *9* (1990) 6763; (b) L. Versluis and T. Ziegler, *J. Am. Chem. Soc.*, *112* (1990) 6763; (c) T. Ziegler, L. Fan, V. Tschinke and A. Becke, *J. Am. Chem. Soc.*, *111* (1989) 2018; (d) A.P.S. Masters, T.S. Sorensen and T. Ziegler, *Organometallics*, *8* (1989) 1088; (e) L. Versluis and T. Ziegler, *Inorg. Chem.*, *29* (1990) 5340; (f) E. Folga and T. Ziegler, *Organometallics*, *12* (1993) 325; (g) T.K. Woo, E. Folga and T. Ziegler, *Organometallics*, *12* (1993) 1289.

24 (a) T. Ziegler, *J. Pure Appl. Chem.*, *63* (1991) 873; (b) T. Ziegler and L. Versluis, *ACS Adv. Chem. Ser.*, *230* (1992) 75; (c) T. Ziegler and V. Tschinke, *ACS Symp. Ser.*, *428* (1990) 277; (d) T. Ziegler, J.G. Snijders and E.J. Baerends, ACS Symp. *Ser.*, *383* (1989) 322; (e) T. Ziegler, V. Tschinke and L. Versluis, *NATO ASI Ser.*, *C176* (1986) 189; (f) T. Ziegler, *NATO ASI Ser.*, *C378* (1992) 367; (g) T. Ziegler, *NATO ASI Ser.*, *C367* (1992) 357.

25 (a) G. Herzberg, *Spectra of Diatomic Molecules*, Van Nostrand Reinholdt, New York, 1950; (b) E.A. Carter and W.A. Goddard, *J. Chem. Phys.*, *88* (1988) 3132; (c) K.M. Ervin, S. Gronert, S.E. Barlow, M.K. Gilles, A.G. Harrison, V.M. Bierbaum, C.H. DePuy, W.C. Lineberger and G.B. Ellison, *J. Am. Chem. Soc.*, *112* (1990) 5750; (d) D.D. Wagman, W.H. Evans, V.B. Parker, R.H. Schuum, I. Halow, S.M. Bailey, K.L. Churney and R.L. Nuttall, *J. Phys. Chem. Ref. Data, Suppl. 2* (1982) 11; (e) J.A. Seetula, Y. Feng, D. Gutman, P.W. Seakins and M.J. Pilling, *J. Phys. Chem.*, *95* (1991) 1658; (f) R. Walsh, *Acc. Chem. Res.*, *14* (1982) 246.